X-ray characteristics of SAX flight mirror units.

G.Conti, E.Mattaini, E.Santambrogio
CNR - Istituto Fisica Cosmica e Tecnologie Relative - Via Bassini 15 - 20133 Milano - Italy
B.Sacco, G.Cusumano
CNR - Istituto Fisica Cosmica con Applicazioni all' Informatica - Via Stabile 172 - 90139 Palermo - Italy
O.Citterio
Osservatorio Astronomico Brera Merate - Via Bianchi 46 - 22055 Merate - Italy
H.Brauninger, W.Burkert
Max Planck Institut für Extraterrestrische Physik - D8046 Garching - Germany

ABSTRACT

The scientific instrumentation onboard the Italian X-ray Astronomy Satellite SAX foresees four X-ray Mirror Units operating in the energy range 0.1-10 KeV with spatial resolution of 1 arcmin Half Power Radius (HPR). The Mirror Units are composed of thirty nested confocal and coaxial very thin double cone mirrors made by a nickel electroforming replica technique. The paper presents the X-ray characterisation data obtained at the PANTER facility on the Flight Mirror Units.

Keywords: X-ray optics, grazing incidence optics.

1. INTRODUCTION

The Italian X-ray Astronomy Satellite SAX [1-3], to be launched at the end of 1995, is a collaborative program between ASI (Italian Space Agency) and NIVR (Netherlands Agency for Aerospace Programs), and includes six scientific instruments, namely

- a Medium Energy Concentrator/Spectrometer (MECS)
- a Low Energy Concentrator/Spectrometer (LECS)
- an High Pressure Gas Scintillation Proportional Counter (HPGSPC)
- a Phoswich Detector System (PDS)
- two Wide Field Cameras (WFC's).

The scientific requirements of the MECS are: an energy range of 1-10 KeV, effective areas of 240 cm^2 and 150 cm^2 at 1 KeV and 7 KeV respectively, a field of view of 30 arcmin with on axis angular resolution of 1 arcmin Half Power Radius at 7 KeV. To fulfil the effective area requirements, with the allowed dimensions of the satellite, the MECS consists of three identical Medium Energy X-ray Telescopes, each composed of a Mirror Unit (MU) and of a Medium Energy Position Sensitive Gas Scintillation Proportional Counter in the focal plane.

The LECS operates in the extended energy range 0.1-10 KeV, with the same field of view and angular resolution as the MECS, and with an effective area of 80 cm^2 at 1 KeV and 50 cm^2 at 7 KeV and consists of a Mirror Unit and of a Position Sensitive Gas Scintillation Proportional Counter with an ultra thin window at the focal plane.

Thus four identical Mirror Units are foreseen onboard of the SAX satellite, each capable of satisfying both MECS and LECS requirements.

The design of the MU was published in a previous paper [4]. Briefly, it is composed of thirty nested coaxial and confocal mirrors having thickness from 0.2 to 0.4 mm. The mirrors have a double cone geometry to approximate the Wolter I configuration, with diameters ranging from 162 to 68 mm, total length of 300 mm and focal length of 1850 mm. Each MU has a weight of about 13 Kg.

A replica technique by nickel electroforming from mandrels was used for making the mirrors [5] and a Development Model of the MU was built at CNR-IFC, Milano. It was tested for X-ray imaging characteristics at the PANTER X-ray facility of Max Plank Institut, Munich [6].

The Engineering Qualification Model MU (EQM) and the four Flight Models MU (FM1-FM4) have been produced by MACDIT, Lecco, in the context of the SAX program, as sub-contractor of LABEN and ALENIA SPAZIO, which is prime contractor for the space segment. The EQM MU was successfully tested and the results were published in a previous paper [7] together with a summary of the mirrors manufacturing and assembling technology. The present paper presents the results of the X-ray tests performed on the Flight Models MUs.

0-8194-1603-7/94/$6.00

2. X-RAY TESTS

The four Flight Models MU were tested at the PANTER X-ray facility of Max Plank Institut für Extraterrestrische Physik, München [8]: FM1, FM2 in August, 93 and FM3, FM4 in January, 94. The test goal was to measure the effective area and the imaging characteristics of the MUs over the whole energy range. The experimental set-up, the test procedure and the data analysis method were the same used for the EQM MU, tested in August 92 [7] and here summarised.

2.1 Experimental set-up

Two MUs are mounted at the same time inside the test chamber and tested independently one after the other. Each MU can be horizontally and vertically tilted in order to align its optical axis with respect to the axis of the X-ray beam. At the focal plane three detectors from MPE are mounted: the engineering model of the ROSAT Position Sensitive Proportional Counter (PSPC) [10], and two identical polypropylene window proportional counters: the first with a circular 25 mm diameter entrance shield (Open Counter), the second one with 100 μm wide vertical slit (Slit Counter). A manipulator allows the centring and the focusing of each detector with respect to the image produced by the MUs. Moreover, the assembly MUs-detectors can be rotated and tilted for off axis measurements. An independent proportional counter, placed at the entrance of the test chamber, is used to monitor the X-ray beam intensity (Monitor Counter).

The measurements were made at 0.3 KeV (C-Kα), 0.9 KeV (Cu-Lα) 1.5 KeV (Al-Lα), 3 KeV (Ag-Lα), 4.5 KeV (Ti-Kα), 6.4 KeV (Fe-Kα), and 8 KeV (Cu-Kα) [9].

A first alignment of the MUs (within few arcmin) inside the test chamber is performed with a divergent He-Ne laser beam that simulate the X-ray beam, looking at the image produced by the direct reflection of the second cone of the innermost mirror. The final adjustment is done at X-ray wavelength with the PSPC detector, using the single reflections that come from the small part of the first cone of all the mirrors, as a consequence of the finite distance of the source (130 m). The PSPC was used also to position the detectors at the best focus of the MUs.

2.2 Effective area

The geometric collecting area of each MU is 123.9 cm^2. The divergence of the X-ray beam causes a loss of area that amounts to 15.7 cm^2. Taking into account the spider obstruction, the geometrical area for the PANTER tests is 97.3 cm^2. The measuring method is described in the EQM paper [7].

At each energy the effective areas were measured on axis and at 5', 10', 15' off axis positions. Table 1 lists the on axis values compared with the *theoretical* ones calculated by ray-tracing simulations (data from EQM model are also listed for comparison). Figures from 1 to 4 show the on axis effective area versus energy for the four Flight Models and Figures 5 and 6 show, as an example, the effective areas versus off axis angle at 0.9, 6.4 and 8 KeV for FM1 and at 1.5, 4.5 and 8 KeV for FM4, together with the calculated curves (solid lines). The experimental data have not been corrected to bring the source to infinity and the ray-tracing are performed with the PANTER configuration.

The gold reflectivity curves versus grazing incidence angle and versus energy, used for the ray-tracing, were derived from Zombek [11]. The error of the measures is ± 5%. To have an estimation of the effective areas with the source at infinity, the reported values must be increased of about 13%.

	0.3 KeV (cm^2)	0.9 KeV (cm^2)	1.5 KeV (cm^2)	3 KeV (cm^2)	4.5 KeV (cm^2)	6.4 KeV (cm^2)	8 KeV (cm^2)
EQM	84.2	81.4	80.9	54.1	57.6	56.9	37.6
FM1	83.0	80.8	81.7	55.4	59.7	56.9	38.3
FM2	82.4	79.2	80.1	54.8	57.7	55.4	36.7
FM3	82.2	79.8	80.6	55.2	58.1	57.9	38.8
FM4	83.2	79.2	80.9	54.7	57.2	57.7	38.9
theory	*84.4*	*82.2*	*82.0*	*47.4*	*58.0*	*53.7*	*37.6*

Table 1 - Measured and theoretical on axis effective areas of SAX EQM and FM Mirror Units.

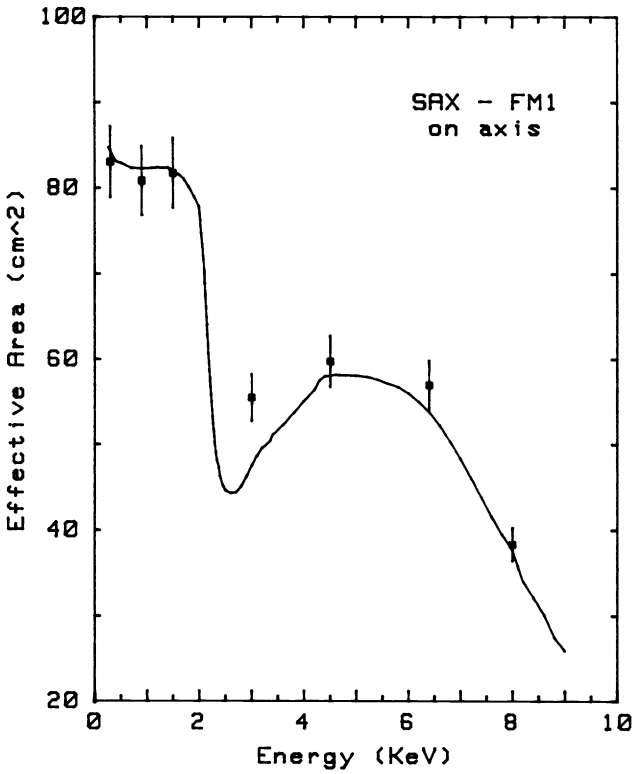

Fig. 1

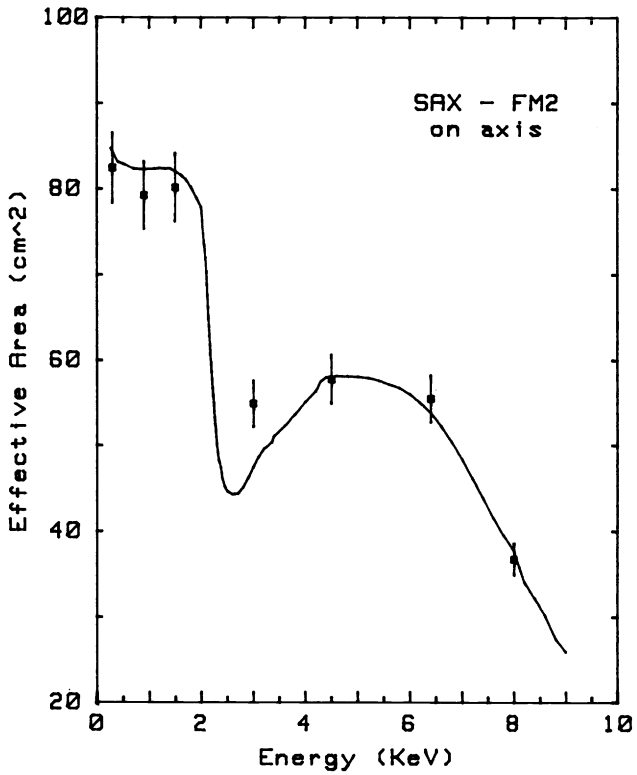

Fig. 2

FM1 / FM2 : measured and theoretical on axis effective areas vs. energy.

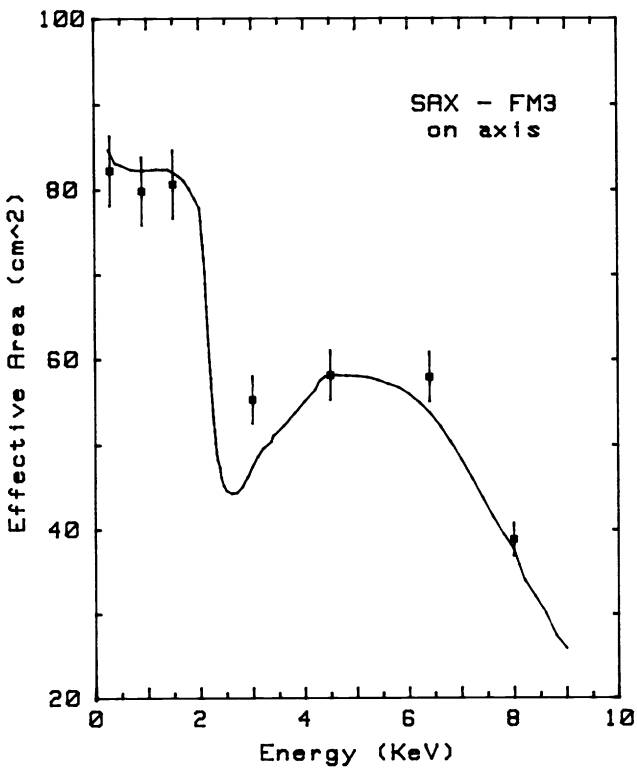

Fig. 3

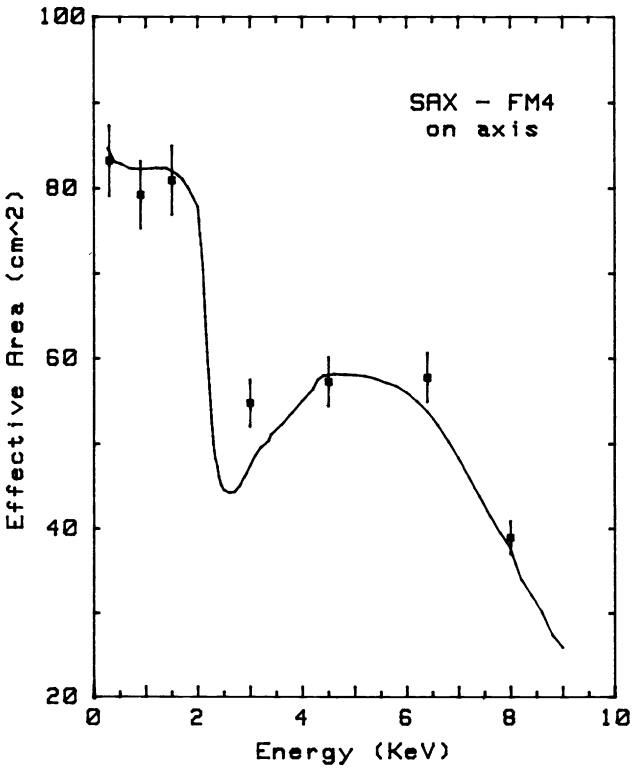

Fig 4

FM3 / FM4 : measured and theoretical on axis effective areas vs. energy.

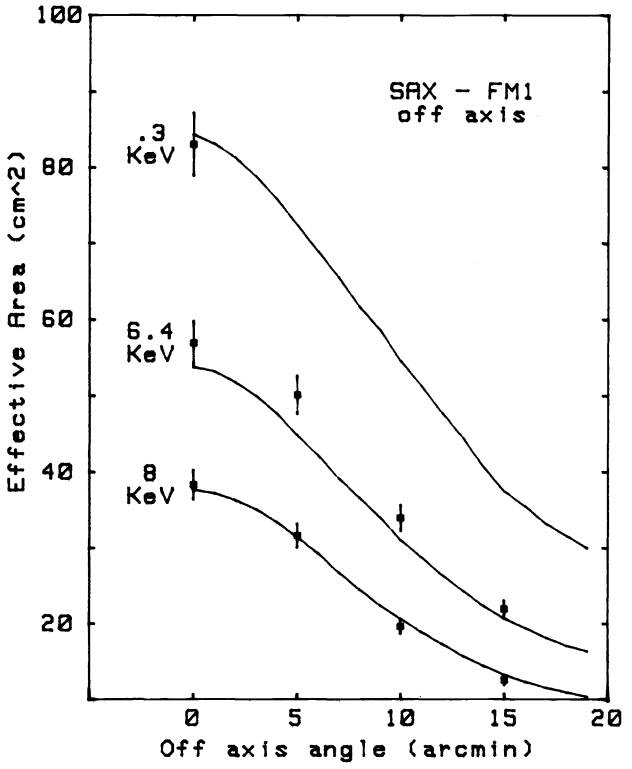

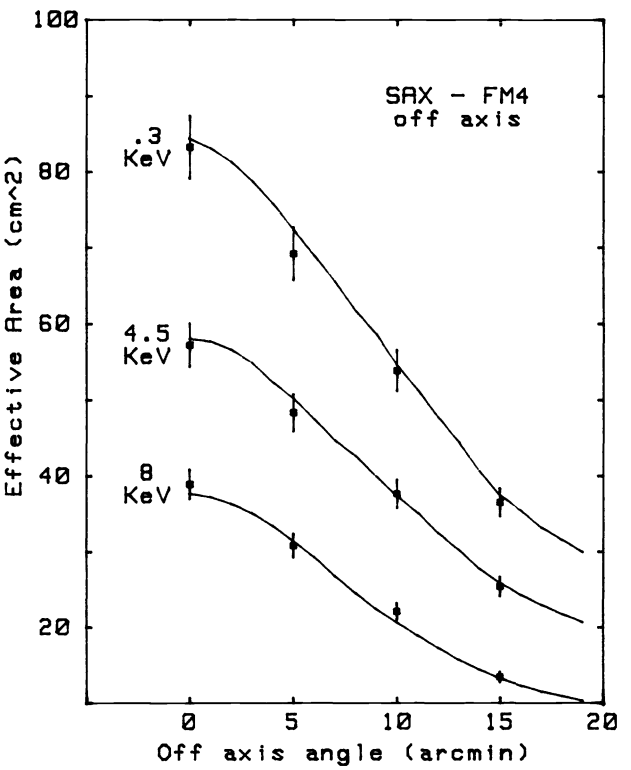

Fig. 5 FM1 / FM4 : measured and theoretical effective areas vs. off axis angle. Fig 6

2.3 Encircled Energy

The imaging characteristics of the four FM MU were measured with the ROSAT PSPC and with the Slit Counter. The PSPC was used, at each energy, to collect on axis images. With the 100 μm Slit Counter, a scan across the on axis image at the focal plane was performed between -12 and 12 mm from the peak for 0.3, 0.9, 1.5 and 3 KeV, and between -15 and 15 mm for 4.5, 6.4 and 8 KeV. The scan step was 50 μm for the 4 mm around the peak and 100 μm for the outer parts; in each position the detector accumulates counts for a fixed time interval.

The Encircled Energy Function (EEF) is the fraction of total energy at the focal plane contained in a circle of radius r, versus r. The EEF is derived by integration from the Point Spread Function (PSF), which is the intensity function of a point source imaged by the MU. The Slit Scan Function (SSF) is the PSF integrated in the direction of the slit. The EEF can be derived directly by integration on a PSPC image but the spatial resolution of the PSPC is energy-dependent. With the hypothesis of a circular symmetry of the image, well verified in our case, the PSF and then the EEF can be derived from the measured SSF: each of them is fitted with the sum of the following four analytical functions, in which G_i and B_i are free parameters of the fit:

$$SSF(x) \rightarrow \sum_{i=1}^{4} G_i/(2B_i(1+(x/B_i)^2)^{3/2})$$

The corresponding PSF is:

$$PSF(r) = \sum_{i=1}^{4} G_i/(\pi B_i^2(1+(r/B_i)^2)^2)$$

which verify the relation

$$\int_{-\infty}^{+\infty} PSF(r)\, dy = SSF(x)$$

because [12] $\int_{-\infty}^{+\infty} G_i/(\pi B_i^2(1+(r/B_i)^2)^2)\, dy = G_i/(2B_i(1+(x/B_i)^2)^{3/2})$ with $r^2=x^2+y^2$

Therefore $EEF(r) = \int_0^{2\pi}\int_0^r PSF(r)\, r\, d\theta dr = \sum_{i=1}^{4} \int_0^{2\pi}\int_0^r rG_i/(\pi B_i^2(1+(r/B_i)^2)^2)\, d\theta dr = \sum_{i=1}^{4} G_i(1-1/(1+(r/B_i)^2))$

Table 2 lists the 50%, 80% and 90% energy radius derived from the slit scan data (results obtained from EQM Model are also reported for comparison) and Fig. 7, 8, 9 and 10 show the Encircled Energy Functions for the FM MUs respectively at 0.3, 1.5, 3 and 8 KeV.

	0.3 KeV			0.9 KeV			1.5 KeV		
	r 50 % ± .2 (arcsec)	r 80 % ± 1.0 (arcsec)	r 90 % ± 3.5 (arcsec)	r 50 % ± .3 (arcsec)	r 80 % ± 1.3 (arcsec)	r 90 % ± 4.0 (arcsec)	r 50 % ± .3 (arcsec)	r 80 % ± 1.5 (arcsec)	r 90 % ± 5.0 (arcsec)
EQM	27.5	61.3	98.5	28.3	63.7	103.7	29.5	67.7	114.1
FM1	27.0	61.3	98.5	-	-	-	28.7	65.8	107.6
FM2	27.2	61.3	98.0	-	-	-	28.8	63.7	101.7
FM3	30.5	71.3	116.9	31.8	72.8	119.1	32.1	75.1	124.1
FM4	32.1	73.5	120.5	31.8	74.0	122.2	33.6	78.9	133.9

	3 KeV			4.5 KeV			6.4 KeV		
	r 50 % ± .3 (arcsec)	r 80 % ± 2.0 (arcsec)	r 90 % ± 7.0 (arcsec)	r 50 % ± .4 (arcsec)	r 80 % ± 2.3 (arcsec)	r 90 % ± 8.5 (arcsec)	r 50 % ± .5 (arcsec)	r 80 % ± 2.5 (arcsec)	r 90 % ± 9.0 (arcsec)
EQM	32.1	76.9	138.7	35.2	90.0	172.5	39.3	106.2	205.0
FM1	32.0	79.6	147.7	34.9	92.2	180.8	40.1	111.5	217.6
FM2	31.7	74.4	129.9	34.2	83.8	153.8	38.4	101.2	198.4
FM3	34.5	84.0	151.4	37.8	103.8	223.5	40.4	111.4	214.7
FM4	35.2	87.2	157.9	38.6	98.9	191.2	41.7	112.0	217.9

	8 KeV		
	r 50 % ± .5 (arcsec)	r 80 % ± 3.0 (arcsec)	r 90 % ± 9.5 (arcsec)
EQM	40.0	110.6	210.7
FM1	42.7	122.1	226.8
FM2	40.6	109.7	212.7
FM3	41.2	113.8	213.4
FM4	40.8	110.8	207.8

Table 2 - Measured 50 % , 80% and 90% Energy Radius of SAX EQM and FM Mirror Units.

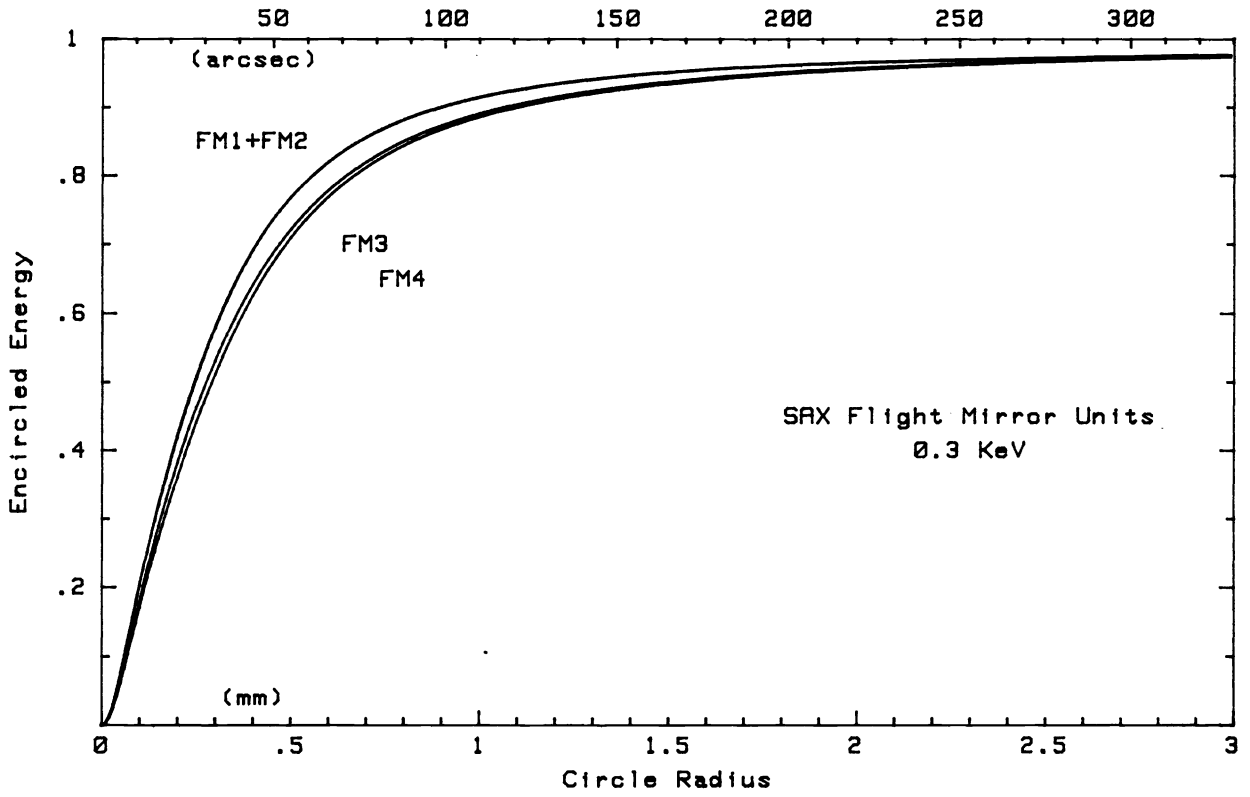

Fig 7 - Encircled Energy Functions at 0.3 KeV.

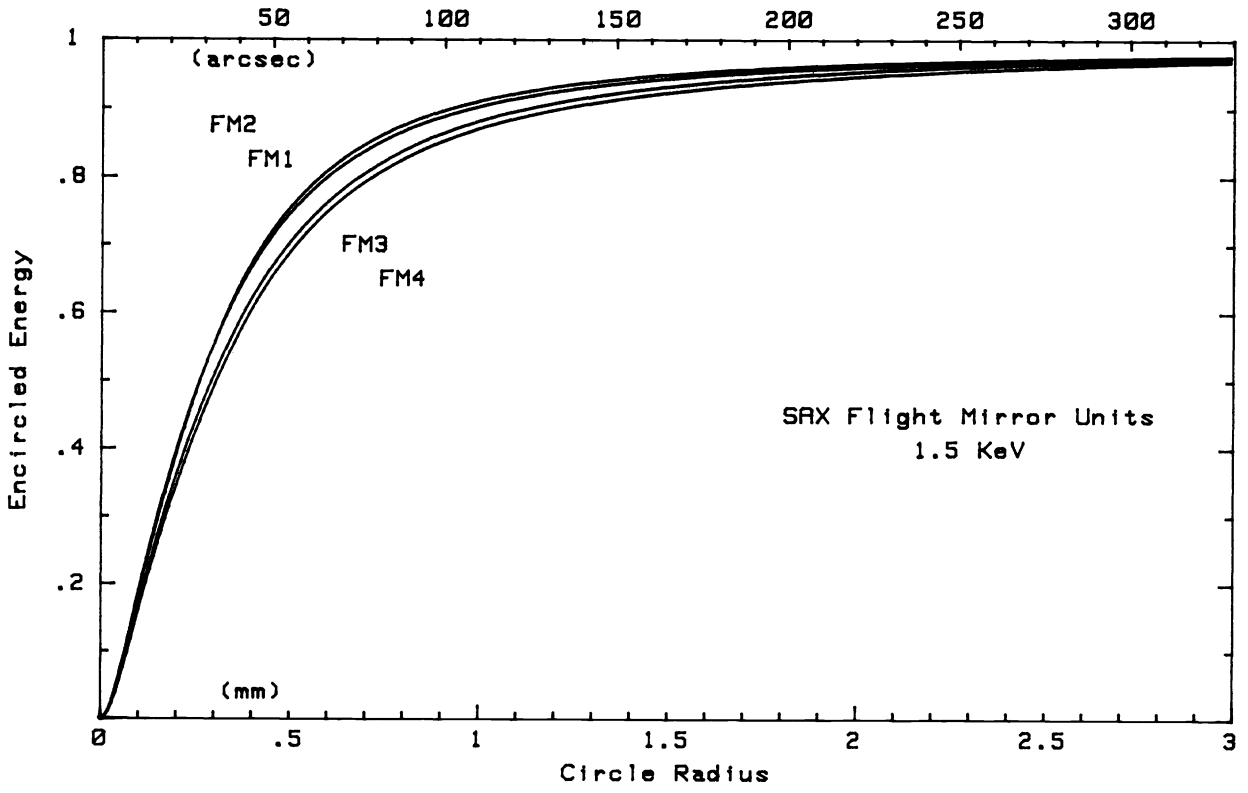

Fig. 8 - Encircled Energy Functions at 1.5 KeV.

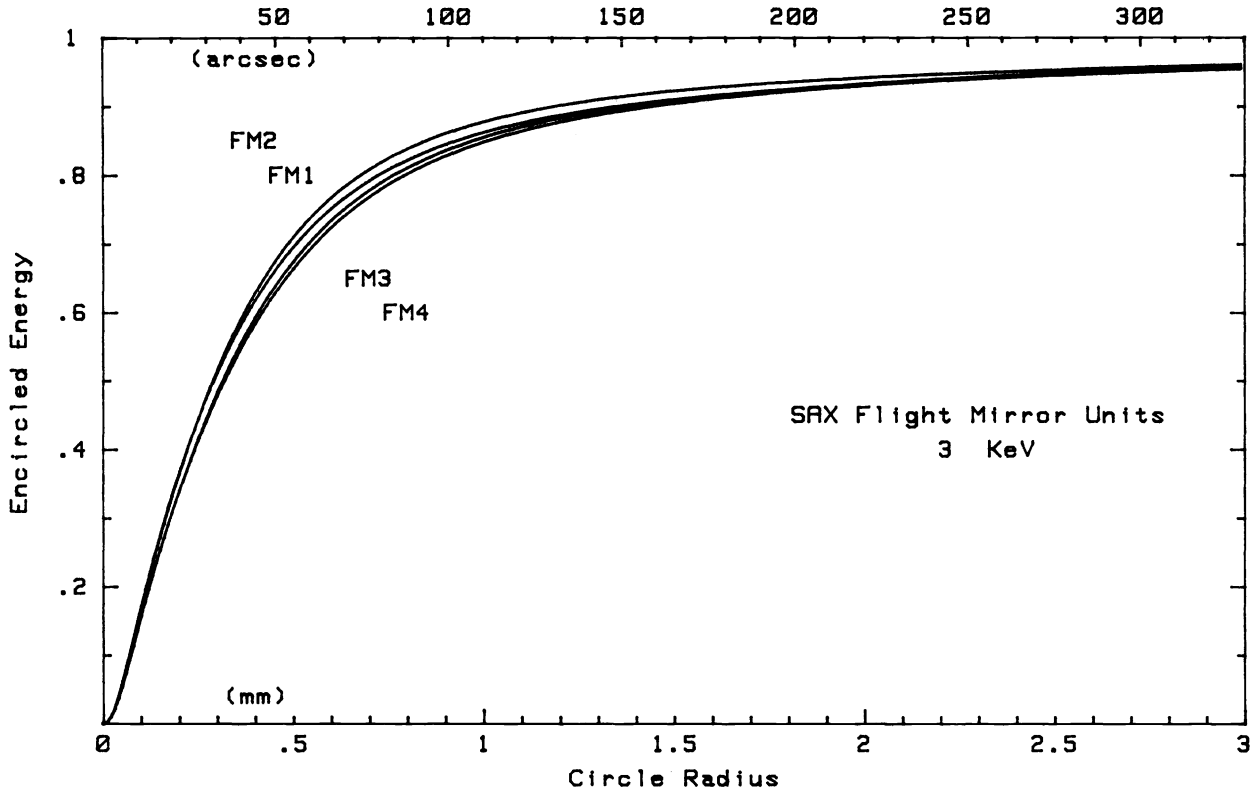

Fig. 9 - Encircled Energy Functions at 3 KeV.

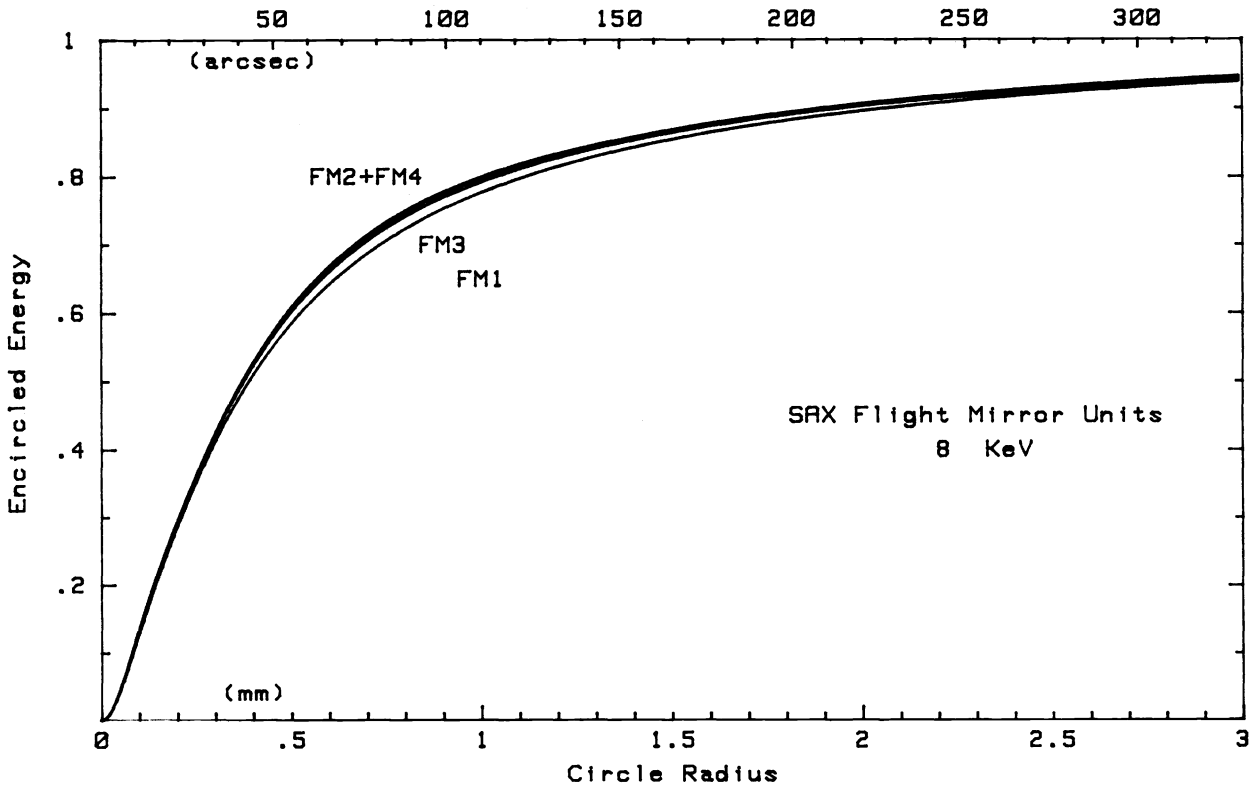

Fig. 10 - Encircled Energy Functions at 8 KeV.

It must be noted that, due to the finite distance of the X-ray source (130 m), 13% of the reflecting surface of the MUs close to the input diameter of the mirrors, that uses for the second reflection a corresponding part near the output of the second cone, does not contribute to the present determination of the Encircled Energy Functions. These parts of the MUs are the ones that interface with the supporting spiders and consequently are likely to be more deformed by the fixation grooves on the spider spokes, giving rise to the so called "marguerite effect" on the focal plane image. Assuming the worste case in which all the photons impinging on these parts of the mirrors are reflected out of a circle of .5 mm radius, and recomputing the HPR (r 50 %), its maximum increase is about 20 % at 8 KeV, well within the specifications of HPR < 60 arcsec.

3. ANOMALOUS RAYS

The off axis behaviour of thirty nested mirrors is quite complicated because "anomalous" rays can reach the focal plane: in addition to the photons that are regularly reflected by the two cones of the mirrors, some rays are reflected by the first or by the second cone only and moreover some other rays can reach the focal plane directly, without reflections. The result of this situation is that photons coming from different angular positions produce ghost images at the focal plane; for X-ray wavelengths and for the SAX MUs the critical reflection angle limits to about 2 degrees the maximum acceptance angle.

It is important to make an evaluation of the contribution that these rays give to the expected background; for this reason the following analysis has been made: starting from 300000 sky photons uniformly distributed on a solid angle of 2 degrees semiaperture, centred on the optical axis of the MU, a ray-tracing simulation has been done with the same model of SAX MU used for theoretical effective area calculations. Table 3 reports the statistics of the "normal" double reflected and "anomalous" X-rays that reach the focal plane. The extragalactic X-ray energy spectrum, which constitutes the most relevant part of the sky background above 1 KeV, has been considered for the simulation.

	counts	%
double reflection	11898	48.3
single reflection (first cone)	6715	27.2
single reflection (second cone)	5612	22.8
no reflection	410	1.7
total	24635	100

Table 3

A simulation with the same starting conditions has also been performed in order to evaluate the ratio between the total counts found in a circle of a given radius at the focal plane and the counts that come from "normal" double reflection. The results are given in Table 4 and do not include the instrumental background. As it can be seen, in a circle of 5 arcmin radius, the increase of the background due to "anomalous" rays is 14 %.

circle radius (arcmin)	ratio
5	1.14
10	1.23
15	1.36
20	1.43

Table 4

4. DISCUSSION AND CONCLUSIONS

The aim of the tests on the flight MUs, the results of which are presented in this paper, was to verify that their own X-ray characteristics were in agreement with the scientific requests. An end to end calibration of the MUs together with the flight models of the detectors (3 MECS and 1 LECS), is planned for the autumn of 94, always at the PANTER X-ray facility.

The measured effective areas fulfil the requirements and are in substantial agreement with the theoretical data, with the exception of the values at 3 KeV which are systematically higher than expected. A possible explanation of this discrepancy is that the continuum contamination of the energy lines has a larger influence at 3 KeV because of the gold absorpion edge; the problem to better characterise the grazing incidence gold coated X-ray optics in the energy range 2-4 KeV is still open.

The angular resolution of 1 arcmin HPR at 7 KeV is well satisfied for all the models, however the measured Encircled Energy Functions require some comments: it is evident that the FM3 and FM4 MUs have worse imaging characteristics than the EQM, FM1 and FM2 models. The difference is mainly present at low energies, which means that it is due to a deformed geometry of the two MU, coming from a worse quality of the mirrors or, more probably, from a deformation induced on the outermost mirrors of the MUs (which give a large contribution to the effective area at low energies), by the assembling spiders; at 6.4 and 8 KeV these mirrors are less efficient and moreover the scattering caused by the roughness of the reflecting surfaces becomes the predominant effect. During the mounting of the reflecting reference cubes on the MUs, which will be the last operation before the final calibrations, it will be possible to have a confirmation of this hypothesis by means of an accurate investigation of the images produced by the MUs at optical wavelength.

The evaluation of the effects of the ghost images on the background has shown that, in a circle of 5 arcmin radius, the increase is no more than 14 %.

ACKNOWLEDGEMENTS

We wish to thank G.Boella and L.Scarsi for supporting and encouraging our work and R.C.Butler, SAX payload manager, for helpful discussions. The technical staff of MACDIT, LABEN and ALENIA SPAZIO industries have given an active collaboration.

REFERENCES

(1) L.Scarsi, "The SAX mission", *Adv. Space Res.* 3, 491 (1984).

(2) G.Spada, "SAX Scientific Instrumentation", *Proc. Conference on "Non thermal and Very High Temperature Phenomena in X-ray Astronomy"*, pp 217-234, Roma (1983).

(3) C.Perola, "The Scientific Objectives of the SAX Mission", *Proc. Conference on "Non thermal and Very High Temperature Phenomena in X-ray Astronomy"*, pp 173-230, Roma (1983) .

(4) O.Citterio, G.Conti, E.Mattaini, B.Sacco and E.Santambrogio, "Optics for X-ray Concentrators on Board the Astronomy Satellite SAX", *Proc. SPIE 597, 102* (1985).

(5) O.Citterio, G.Bonelli, G.Conti, E.Mattaini, E.Santambrogio, B.Sacco, E.Lanzara, H.Brauninger and W.Burkert, "Optics for the X-ray Imaging Concentrators Aboard the X-ray Astronomy Satellite SAX", *Appl. Opt. 27, 1470* (1988)

(6) O.Citterio, P.Conconi, G.Conti, E.Mattaini, E.Santambrogio, G.Cusumano, B.Sacco, H.Brauninger and W.Burkert, "Imaging Characteristics of the Development Model of the SAX X-ray Imaging Concentrator", *Proc. SPIE 1343, 145* (1990).

(7) G.Conti, E.Mattaini, E.Santambrogio, B.Sacco, G.Cusumano, O.Citterio, H.Brauninger and W.Burkert, "Engineering Qualification Model of the SAX X-ray Mirror Unit. Technical data and X-ray Imaging Characteristics", *Proc. SPIE 2011, 118* (1993).

(8) B.Aschenbach, H.Brauninger, K.H.Stephan and J.Trumper, "X-Ray Test Facilities at Max Planck Institute, Garching", *Proc. SPIE 184, 234* (1979).

(9) K.H.Stephan, P.Predhel, B.Aschenbach, H.Brauninger and A.Ondrusch, "Soft X-ray Source for the Max Planck Institute (MPI) Long Beam (130 m) Test Facility", *Proc. SPIE 316, 203* (1981).

(10) U.Briel and E.Pfefferman", The Position Sensitive Proportional Counter (PSPC) of the ROSAT Telescope", *Nucl. Instr. and Meth. A242 , 376* (1986).

(11) M.V.Zombek, *AXAF Interim Rep. SAO-AXAF016* (1983).

(12) I.S. Gradshteyn and I.M. Ryzhyk, *Tables of Integrals, Series, and Products*, p. 294, 3.249, Academic Press (1980).